# Surface Tension and Density of Oxygen-Free Liquid Aluminum at High Temperature

**V. Sarou-Kanian,**[1,2] **F. Millot,**[1] **and J. C. Rifflet**[1]

New values of densities $\rho$ and surface tensions $\sigma$ of liquid aluminum obtained in the range 1600 to 2360 K by contactless techniques in neutral gases are reported. Conditions for oxygen-free aluminum are fulfilled which allow determination of the surface tension of aluminum. Extrapolation to the melting point, $T_m = 933$ K, confirms the value of $\sigma$ ($T = 933$ K) = 1.05 N·m$^{-1}$.

## 1. INTRODUCTION

The surface tension and density of liquid aluminum have been widely studied in the past. Although we expect the density to be quite well known, the surface tension may be more sensitive to environmental effects because of the great affinity of aluminum for oxygen. A detailed review paper on the surface tension of metals by Keene [1] indicates, for example, differences on the order of 25% between most data and the few results obtained on "pure Al" [2–4] near the melting point. These isolated results have not been confirmed up to now because of the experimental difficulty of producing oxygen-free surfaces of liquid aluminum.

In the meantime, new experimental techniques have emerged that allow measurement of the density and surface tension up to 3000°C [5, 6]. These promising techniques are applied to liquid aluminum in this paper because the difficulty of obtaining oxygen-free aluminum surfaces at low

---

[1] Centre de Recherches sur les Matériaux à Haute Température, CNRS, 1D avenue de la Recherche Scientifique, 45071 Orléans cedex 2, France.

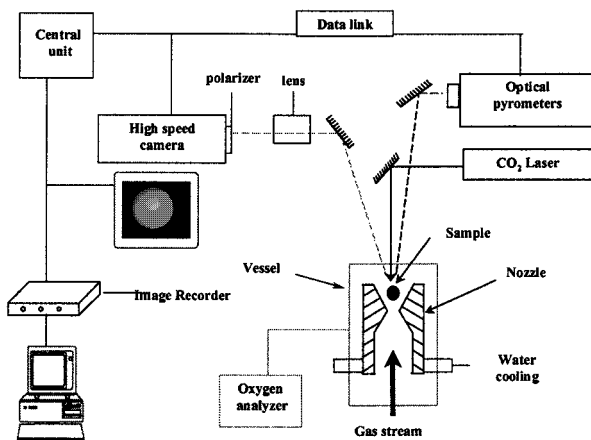[2] To whom correspondence should be addressed. E-mail: sarou@cnrs-orleans.fr

**Fig. 1.**   Experimental setup.

temperature is overcome at high temperature by using a facility for removing oxygen from an Al surface by forming $Al_2O^{(gas)}$ in a neutral or reducing atmosphere [7–10].

## 2. EXPERIMENTAL

The experimental setup is shown in Fig. 1. It consists of maintaining a liquid aluminum drop, heated with a 800 W $CO_2$ laser, on a gas flow of about $1 \ell \cdot min^{-1}$ in a convergent/divergent nozzle. This nozzle is made of aluminium, and it is water-cooled. This setup has been successfully used in the recent past on oxides [5, 11] as well as on liquid iron [12], liquid nickel, or liquid boron [6, 13]. The size of drops between 1 and 5 mm and the powerfulness of $CO_2$ laser help to maintain liquids in stable levitation on almost any gas at temperatures that can be as high as 3000°C [5]. The laser beam which has a size of 1 cm in diameter, heats the few mm-sized drops directly and also after reflection on the nozzle. The asymmetric heating induces a small temperature gradient in the liquid drop, which depends on the thermal conductivity and total emissivity of the drop. Song and Li [14] have presented a numerical analysis of this problem for levitated drops and applied it to various liquid metallic drops having diameters of 1.8 mm. They have shown, for example, that a liquid iron drop heated with a $CO_2$ laser at $T = 1900$ K has an inhomogeneity of temperature of 15 K. This last value is higher than that expected for aluminum drops of the same size and at the same temperature because the thermal conductivity K and total hemispherical emissivity $\varepsilon$ of aluminum

$(K(Al) = 95 \ W \cdot m^{-1} \cdot K^{-1}$ [15] and $\varepsilon = 0.2$ [16]) are more favorable than those of iron $(K(Fe) = 78 \ W \cdot m^{-1} \cdot K^{-1}$ [14] and $\varepsilon = 0.3$ [16]).

Drops of masses between 20 and 50 mg were obtained from Al chips from Goodfellow (purity grade 99.99%). The gases that have been used to levitate the drops were Ar and He, as well as a gas mixture $Ar + 10\% H_2$. A system for purification of rare gases made of TiZr chips heated at 750°C is placed in the gas stream just before the levitation nozzle. An oxygen analyzer made of an electrolytic cell, $(Pd, PdO)/(ZrO_2, Y_2O_3)/(analyzed gas)$ working at $T = 800$ K, was used to determine gas composition at the outlet of the experimental chamber.

Values of $\frac{p_{H_2O}}{p_{H_2}} \leqslant 10^{-3}$ were obtained for purified rare gases, and correspondingly $p_{H_2O} \leqslant 10^{-8}$ bar. The gas mixtures of $Ar + 10\% H_2$, which were not purified, contained approximately 10 ppm $H_2O$.

A three-color pyrometer operating at wavelengths of 0.4, 0.55, and 0.8 μm was used to determine the temperature of the drop. It was first calibrated at the melting point of a compound of known emissivity. The temperature of the liquid aluminum drops was then obtained with the three pyrometers assuming an emissivity value of 0.09 at 1550 K following Krishnan and Nordine [10].

A high-speed CCD camera Kodak Ektapro 1000HRColor ($512 \times 384$ pixels, 8 bit coding, 1000 Hz speed of 2730 frames) equipped with a telecentric optical setup is used to get images of the drop which are then analyzed to determine the geometrical properties of the drop, area, diameters, and geometrical center, as already described [5, 11–13].

A weighted piece of aluminum is placed in the nozzle and heated progressively with the $CO_2$ laser. Formation of the drops occurs at the melting temperature of 933 K. Alumina floating on the surface of the aluminum drop is easily detected by visual observation because its emissivity is ten times larger than that of aluminum. During heating of the drop, alumina is observed systematically on the surface of the liquid at temperatures lower than 1600 K as shown in Fig. 2. When the temperature becomes higher, evaporation of the drop becomes more important and liquid alumina disappears from the Al surface because of chemical reactions between Al and $Al_2O_3$ to form $Al_2O^{(gas)}$ which is taken away by the neutral or reducing levitation gas flow. These observations have already been reported by Krishnan and Nordine [10] at 1900 K in pure He and also by Laurent *et al.* [8] at 1000 K in vacuum. A thermodynamic explanation of this purification process has been reported by Brewer and Rosenblatt [7]. At 2000 K, for example, the partial pressure of $Al_2O^{(gas)}$ in equilibrium with Al and $Al_2O_3$ is $p_{Al_2O} = 5 \times 10^{-3}$ while the aluminum partial pressure is $p_{Al} = 6 \times 10^{-3}$ bar [18]. The overall O/Al atomic ratio in the pure rare gas in equilibrium with the $Al/Al_2O_3$ mixture at 2000 K is $(\frac{O}{Al})^{(g)} = \frac{p_{Al_2O}}{2p_{Al_2O} + p_{Al}}$.
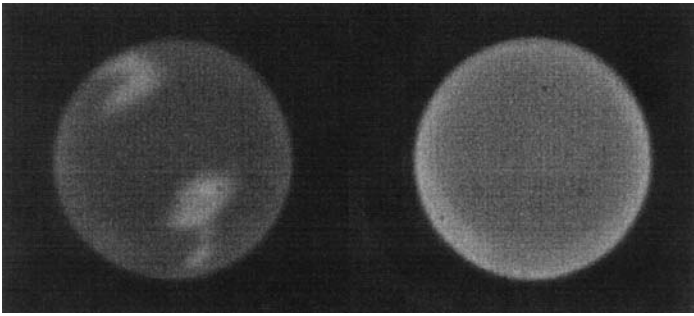
**Fig. 2.** Images of aluminum drop heated at two different temperatures in a purified argon flow: Left, at lower temperature alumina (bright spots) is floating on liquid aluminum. Right, at higher temperature the aluminum surface is alumina free.

This value is much higher than the corresponding value in the liquid aluminum saturated with oxygen at 2000 K, $(\frac{O}{Al})^{(\ell)} = 0.025$ [17], and this explains the mechanism of purification. Brewer and Rosenblatt [7] have also shown that there exists a limiting value of the ratio $(\frac{O}{Al})^{(g)}/(\frac{O}{Al})^{(\ell)} = 48$ when the overall pressure of oxygen is reduced. Taking, for example, $p_{Al_2O} = 10^{-5}$ corresponding to the reduction of available oxygen in the gas flow by aluminum, we get $(\frac{O}{Al})^{(\ell)} = 4 \times 10^{-5}$. Under our experimental conditions, this value is an upper limit.

The density can be easily determined if the deviation from a spherical shape is negligible. A calibration is first performed which consists of recording images of an alumina spherical drop (from Precision Ball and Gauge Co.) of known size ($\Phi = 3 \pm 0.001$ mm) at room temperature. An experiment in under the same optical conditions on liquid aluminum permits, after cooling and weighing the drop of mass $m$, a determination of the liquid density $\rho$ from the measured surface area A:

$$\rho = \frac{3m}{2\pi^{1/2} A^{3/2}} \tag{1}$$

The precision of the density values is dependent on the validity of the approximation of the sphericity of the drop and on the various sources of error involved during the measurement. We have already discussed this question in detail for the case of the measurement of the density of liquid alumina [5]. It had been shown from experiment that significant deviations ($> 1\%$) of the apparent density due to the deviation from sphericity was observed for drops weighing more than 78 mg. These conclusions apply to

aluminum because the deviation from sphericity is directly dependent on the mass, the surface tension, and the density of drops which are similar for aluminum ($\sigma \approx 0.7 - 0.8$ N·m$^{-1}$ and $\rho \approx 2000$ kg·m$^{-3}$) and for alumina ($\sigma \approx 0.65$ N·m$^{-1}$ and $\rho \approx 2800$ kg·m$^{-3}$). The uncertainties coming from the setup may induce a systematic error of 1.5% in the density results.

The surface tension is deduced from the surface oscillations. The surface oscillations are continuously excited by the gas stream in the nozzle which amplifies its natural vibration modes. As a matter of fact, it is a three-dimensional (3D) harmonic oscillator because surface tension acts as the force that makes the drop have a spherical shape. We have already analyzed the oscillation spectrum of a rotating and precessing drop having a small static deformation [6]. An example of such Fourier transforms of the area and the difference ($D_0 - D_{90}$) of two perpendicular diameters of an Al drop are shown in Fig. 3. We observe five domains of frequencies showing vibrations at 120, 139, 151, 162, and 167 Hz. The peaks at $v_{-2} = 120$ Hz and $v_{+2} = 167$ Hz appear in the $D_0 - D_{90}$ spectrum because they correspond to a mode of vibration corresponding to elliptical oscillations without apparent surface change whereas the peak $v_0 = 151$ Hz is the main peak of the area spectrum because it signifies another mode of vibration corresponding to area oscillations with no change of ellipticity. The two last peaks $v_{-1} = 139$ Hz and $v_{+1} = 162$ Hz are weak peaks in both spectra and correspond to a third vibration mode having oscillations of ellipticity and area at the same time.
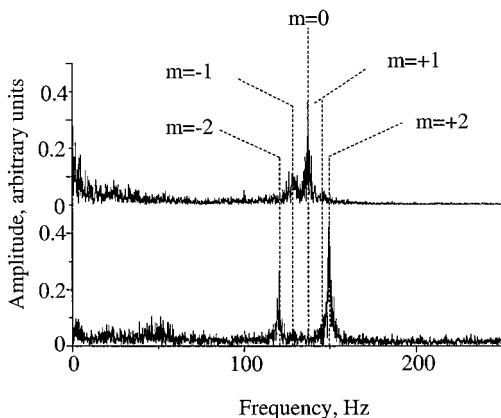


**Fig. 3.** Fourier transforms of area (upper curve) and Fourier transform of the difference of two perpendicular diameters (lower curve) of 2048 image sequence recorded at 500 Hz on a 36.69 mg liquid aluminum drop at 1792 K.

The spectra of Fig. 3 are complicated by the kinematic effects induced by rotation and precession. The vibration modes corresponding to elliptical oscillations are split into two frequencies obeying the relations:

$$\nu_{+1} - \nu_{-1} = 2\Omega_R \qquad \text{and} \qquad \nu_{+2} - \nu_{-2} = 4\Omega_R \qquad (2-3)$$

where $\Omega_R = 11.5$ Hz is the rotation frequency.

The precession frequency $\Omega_P$ is approximately 1 Hz, which is the difference of frequency between the maximum of $\nu_1$ on $D_0 - D_{90}$ and area FFTs of Fig. 2. It is also responsible for the shape of the frequency domains in Fig. 3 because it transforms a single vibration peak in a series of peaks under a Gaussian envelope.

The surface tension $\sigma$ is directly deduced from frequencies and the mass $m$ of the drop;

$$\sigma = \frac{\pi m}{8} \left( \nu_0^2 + \left( \frac{\nu_{-1}^2 + \nu_{+1}^2}{2} \right) + \left( \frac{\nu_{-2}^2 + \nu_{+2}^2}{2} \right) \right) \qquad (4)$$

The precision of the surface tension is dependent on the precision of the frequency ($\pm 0.25$ Hz) and mass ($\pm 10$ μg) determinations and is of the order of 2%.

## 3. RESULTS

Results for the density are shown in Fig. 4 and compared with earlier data [19–28]. The two curves represent the density evaluated during the free cooling of two drops between 1700 and 2200 K. Note that in order to eliminate the fluctuations of the density induced by the vibrations of the drop (surface tension), these two curves were smoothed with a FFT filter (band block = vibration frequencies).

Evaporation of aluminum becomes important above 2200 K and, thus, few results between 2000 and 2360 K were deduced from the last picture obtained with the camera before the drop crashed on the water-cooled nozzle (symbols A to D in Fig. 4).

Our data obtained between 1639 and 2360 K show little scatter. Comparisons with literature results are limited to a few data reported for temperatures higher than 1600 K. These few data [23] are in good agreement with the results of this study. The complete set of data in Fig. 4 can be well represented by a linear function of temperature: $\rho(10^3 \text{ kg} \cdot \text{m}^{-3}) = 2.4 - 0.0003(T(K) - 933)$ as shown in Fig. 4 (dashed line). Other density data [28–30], which, for clarity, are not shown in Fig. 3, are also in reasonable agreement with this equation.
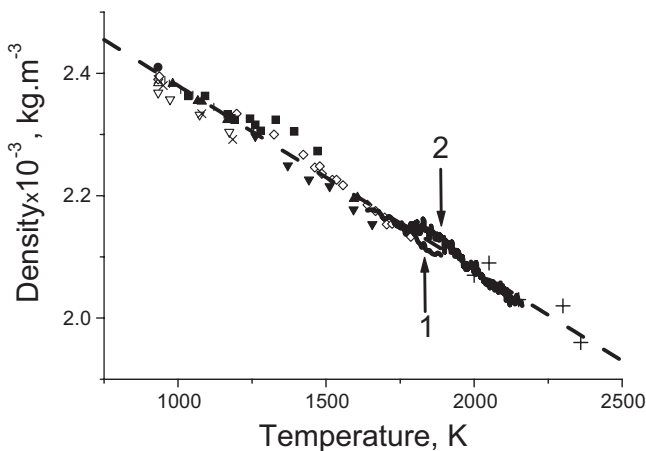
**Fig. 4.** Density of liquid aluminum versus temperature: curves 1 and 2, this work (free cooling), [+] this work, ● [19], △ [20], ▽ [21], × [22], ◇ [23], ▼ [24], ▲ [25], | [26], ■ [27], (- - -) dashed line through data.

Results for the surface tension are shown in Fig. 5. Our results are represented by the points between 1790 and 2170 K and by the dotted line deduced from a linear fit of experimental values as a function of temperature: $\sigma(\text{mN} \cdot \text{m}^{-1}) = (1024 \pm 48) - (0.274 \pm 0.025)(T(K) - 933)$. There is no influence of the gas (He, Ar/H$_2$, or Ar) used to obtain the data.

## 4. DISCUSSION

The present work extends knowledge of the density and the surface tension of liquid aluminum to high temperature. In order to compare the new results with the data already reported in the literature at lower temperature (see Figs. 4 and 5), we need to examine the sources of uncertainties in the determination of the temperature.

The temperature was determined with a three-wavelength pyrometer assuming a temperature and wavelength independent emissivity of $0.09 \pm 0.01$ for liquid aluminum. This convenient temperature scale, based on the emissivity of liquid aluminum determined at 1550 K by Krishnan and Nordine (Fig. 5 of Ref. 10), can introduce some error in the temperature values. In order to precisely determine this point, we have calculated the normal spectral emissivities of aluminum between 1300 and 1800 K from the index of refraction $n$ and the extinction coefficient $k$ determined by
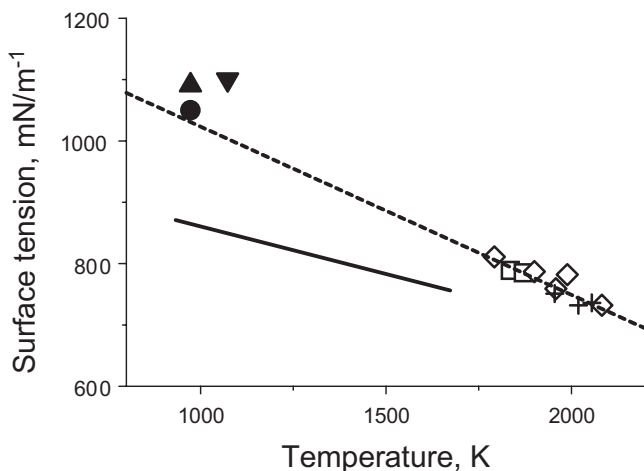
**Fig. 5.** Surface tension of liquid aluminum versus temperature: ● [3], ▲ [4], ▼ [2], ◇ in Ar + 10% H$_2$, □ in He, + in purified argon, this work. Dotted line: linear fit to our data, solid line: compilation of Keene [1].
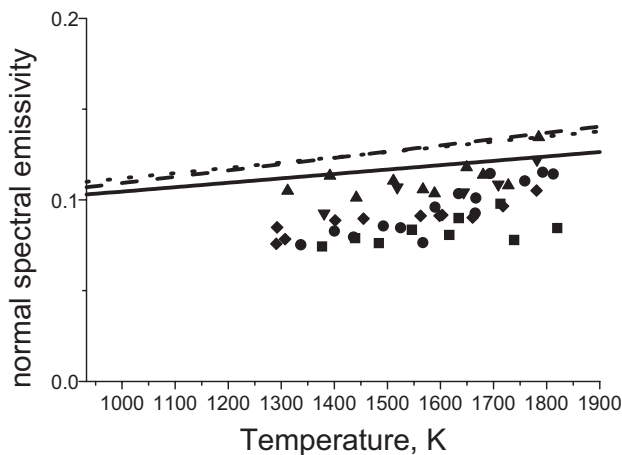


**Fig. 6.** Normal spectral emissivity of liquid aluminum at wavelength $\lambda$ following the experimental work of Krishnan and Nordine [10] ( $\lambda = 381$ nm (■), $\lambda = 422$ nm (●), $\lambda = 500$ nm (▲), $\lambda = 625$ nm (▼), $\lambda = 968$ nm (♦)) and following the model of Hüttner [31] ($\lambda = 355$ nm (---), $\lambda = 530$ nm (···), $\lambda = 1064$ nm (—)).

Krishnan and Nordine [10] at 5 different wavelengths. The emissivities were represented as $\varepsilon(\lambda, T) = 1 - [(n-1)^2 + k^2]/[(n+1)^2 + k^2]$, and they are plotted in Fig. 6.

From this figure, the general trend is that the emissivity increases with temperature for wavelengths between 381 and 968 nm. The same conclusion is reached from a semi-phenomenological theory of metals, using only one fitting parameter published by Hüttner [31] whose predictions for emissivity are reported in Fig. 6. In another paper, Krishnan and Nordine [32] have deduced that their experimental data at 1550 K could be accurately described by a four-parameter Ashcroft-Sturm model, which is an upgraded version of the model of Hüttner. The temperature coefficient of the emissivities proposed by Hüttner [31] is in the range $\frac{d\sigma}{dT} = (3 \pm 0.5) \times 10^{-5} \, \text{K}^{-1}$ and that from the data of Krishnan and Nordine [10] is in the range $(3 \text{ to } 9 \pm 2) \times 10^{-5} \, \text{K}^{-1}$, depending on the wavelength. From the first number, the temperature correction is approximately $\Delta T = 0$ K at 1500 K and $\Delta T = -27 \pm 6$ K at 2000 K, depending on the wavelength of the pyrometer. The slope of the density data as a function of the temperature changes from 0.3 to 0.31 $\text{kg} \cdot \text{m}^{-3} \cdot \text{K}^{-1}$, and the slope of the surface tension versus temperature from 0.274 to 0.290 $\text{mN} \cdot \text{m}^{-1} \cdot \text{K}^{-1}$, the fitting line in this last case just intercepts the lower point of 1.05 $\text{N} \cdot \text{m}^{-1}$ obtained on pure aluminum by Goumiri and Joud [3].

## 5. CONCLUSIONS

The values reported here of the density and the surface tension of liquid aluminum between 1600 to 2300 K extend the data reported in the literature to higher temperatures. Temperature variations of density are correctly represented by a straight line from 933 to 2360 K, the slope of which is 0.3 to 0.31 $\text{kg} \cdot \text{m}^{-3} \cdot \text{K}^{-1}$, depending on the choices made for the emissivity of aluminum. Surface tension values obtained on oxygen free aluminum between 1600 and 2100 K are well represented by a linear fit as a function of temperature that extrapolates through previous data obtained in oxygen-free conditions near the melting point to $\sigma = 1.05 \, \text{N} \cdot \text{m}^{-1}$. This value agrees with the results of a few groups, which is in contrast with most data near 0.870 $\text{N} \cdot \text{m}^{-1}$ at the same temperature.

## REFERENCES

1. B. J. Keene, *Int. Mater. Rev.* **38**:157 (1993).
2. C. Garcia-Cordivilla, E. Louis, and A. Pamies, *J. Mater. Sci.* **21**:2787 (1986).

 3. L. Goumiri and J. C. Joud, *Acta Metall.* **30**:1397 (1982).
 4. A. Pamies, C. Garcia-Cordovilla, and E. Louis, *Scr. Metall.* **18**:869 (1984).
 5. B. Glorieux, F. Millot, J. C. Rifflet, and J. P. Coutures, *Int. J. Thermophys.* **20**:1085 (1999).
 6. F. Millot, J. C. Rifflet, G. Wille, V. Sarou-Kanian, and B. Glorieux, *J. Amer. Ceram Soc.* **85**:187 (2002).
 7. L. Brewer and G. M. Rosenblatt, *Trans. Metall. Soc. AIME* **224**:1268 (1961).
 8. V. Laurent, D. Chatain, C. Chatillon, and N. Eustathopoulos, *Acta Metall.* **36**:1797 (1988).
 9. S. Krishnan, J. K. R. Weber, P. C. Nordine, R. A. Schiffman, R. H. Hauge, and J. L. Margrave, *High Temp. Sci.* **30**:137 (1991).
10. S. Krishnan and P. C. Nordine, *Phys. Rev. B* **47**:11780 (1993).
11. B. Glorieux, F. Millot, and J. C. Rifflet, *Int. J. Thermophys.* **23**:1249 (2002).
12. G. Wille, F. Millot, and J. C. Rifflet, *Int J. Thermophys.* **23**:1197 (2002).
13. F. Millot, J. C. Rifflet, V. Sarou-Kanian, and G. Wille, *Int J. Thermophys.* **23**:1185 (2002).
14. S. P. Song and B. Q. Li, *Int. J. Heat Mass Transfer* **43**:3589 (2000).
15. R. E. Taylor, H. Groot, T. Goerz, J. Ferrier, and D. L. Taylor, *High Temp. High Press.* **30**:169 (1998).
16. Y. S. Touloukian and D. P. DeWitt, *Thermophysical Properties of Matter*, Vol. 7 (IFI/Plenum, New York, 1970), p. 24a.
17. S. Otsuka and Z. Kozuka, *Trans. Jap. Inst. Met.* **22**:558 (1981).
18. M. W. Chase, Jr., C. A. Davies, J. R. Downey, Jr., D. J. Frurip, R. A. Mc Donald, and A. N. Syverud, JANAF Thermochemical Tables, 3rd Ed., *J. Phys. Chem. Ref. Data* **14**:177 (1985).
19. P. Pascal and A. Jouniaux, *Acad. Sci. Paris* **158**:414 (1914).
20. J. D. Edwards and T. A. Moorman, *Chem. Met. Eng.* **24**:61 (1921).
21. E. Gebhardt, M. Becker, and S. Dorner, *Aluminum*, **31**:315 (1955).
22. W. J. Coy and R. S. Mateer, *Trans. ASM* **58**:99 (1965).
23. E. S. Levin and G. D. Ayushina, *Teoplofiz. Vys. Temp.* **6**:432 (1968).
24. E. I. Gol'tsova, *Teplofiz. Vys. Temp.* **3**:483 (1965).
25. J. E. Elliott and M. Gleiser, *Thermochemistry for Steelmaking* (Addison–Wesley, London, 1960).
26. V. M. Glazov and Yu. D. Chistykov, *Akad. Nauk. SSSR, Otdel. Tekhn. Nauk* **7**:141 (1958).
27. V. N. Eremenko, V. I. Nizhenko, and Yu. V. NaidichIzv, *Akad. Nauk SSSR, Odtel. Tekhn. Nauk, Metallurgiya i Toplivo* **3**:150 (1961).
28. N. A. Vatolin, O. A. Esin, V. F. Ukhov, and E. L. Dubinin, *Trudy Inst. Met. Sverdlovsk* **18**:73 (1969).
29. P. M. Smith, J. W. Elmer, and G. F. Gallegos, *Scr. Mater.* **40**:937 (1999).
30. S. P. Yatsenko, V. I. Kononenko, and A. L. Sukhman, *High Temp.* **10**:55 (1972).
31. B. Hüttner, *J. Phys. Condens. Matter.* **4**:2459 (1994).
32. S. Krishnan and P. C. Nordine, *Phys. Rev. B* **48**:4130 (1993).